

2008

# Nonthermal Laser-Induced Formation of Crystalline Ge Quantum Dots on Si(100)

M. S. Hegazy  
*Old Dominion University*

H. E. Elsayed-Ali  
*Old Dominion University, [helsayed@odu.edu](mailto:helsayed@odu.edu)*

Follow this and additional works at: [https://digitalcommons.odu.edu/ece\\_fac\\_pubs](https://digitalcommons.odu.edu/ece_fac_pubs)

 Part of the [Atomic, Molecular and Optical Physics Commons](#), [Electronic Devices and Semiconductor Manufacturing Commons](#), [Quantum Physics Commons](#), and the [Semiconductor and Optical Materials Commons](#)

## Repository Citation

Hegazy, M. S. and Elsayed-Ali, H. E., "Nonthermal Laser-Induced Formation of Crystalline Ge Quantum Dots on Si(100)" (2008). *Electrical & Computer Engineering Faculty Publications*. 100.  
[https://digitalcommons.odu.edu/ece\\_fac\\_pubs/100](https://digitalcommons.odu.edu/ece_fac_pubs/100)

## Original Publication Citation

Hegazy, M. S., & Elsayed-Ali, H. E. (2008). Nonthermal laser-induced formation of crystalline Ge quantum dots on Si(100). *Journal of Applied Physics*, 104(12), 124302. doi:10.1063/1.3041493

# Nonthermal laser-induced formation of crystalline Ge quantum dots on Si(100)

M. S. Hegazy and H. E. Elsayed-Ali<sup>a)</sup>

*Department of Electrical and Computer Engineering and the Applied Research Center, Old Dominion University, Norfolk, Virginia 23529, USA*

(Received 16 July 2008; accepted 29 October 2008; published online 17 December 2008)

The effects of laser-induced electronic excitations on the self-assembly of Ge quantum dots on Si(100)-(2×1) grown by pulsed laser deposition are studied. Electronic excitations due to laser irradiation of the Si substrate and the Ge film during growth are shown to decrease the roughness of films grown at a substrate temperature of ~120 °C. At this temperature, the grown films are nonepitaxial. Electronic excitation results in the formation of an epitaxial wetting layer and crystalline Ge quantum dots at ~260 °C, a temperature at which no crystalline quantum dots form without excitation under the same deposition conditions. © 2008 American Institute of Physics. [DOI: 10.1063/1.3041493]

## I. INTRODUCTION

Electronic excitations by laser or electron beam interaction with surfaces have been shown to modify the surface properties.<sup>1–5</sup> Electronic-induced surface processes include selective removal of surface atoms, surface layer modifications, and the alternation of rates of some surface processes.<sup>6</sup> Removal of surface atoms occurs due to bond breaking as a result of single or multiple photon excitations. In semiconductors, bond breaking by laser pulses below the melting threshold is purely electronic.<sup>7</sup> Even what was thought of as purely thermal desorption was reported to involve electronic excitations.<sup>8</sup>

In Si(100)-(2×1), bond breaking takes place due to the localization of two photo-generated surface holes at dimer sites.<sup>7</sup> Two-hole localization (THL) on surface sites of non-equilibrated valance holes was concluded to be the mechanism responsible for bond breaking when a Si(111)-(2×1) surface was excited by 1064 nm, 3.5 ns laser pulses.<sup>9</sup> The number of the electronically removed atoms due to laser excitations depends on the laser wavelength and is a superlinear function of laser fluence, but is independent of the material's temperature.<sup>5,6</sup>

A few publications have considered the effects of the electronic excitations on the growth of thin films and nanostructures. Illumination of silica substrates with a low-fluence diode laser during deposition has been reported to unify the cluster's shape and narrow the size distribution of Ga nanoparticles grown at ~100 °C.<sup>10</sup> Recently, our group has achieved homoepitaxy of Si(111)-(7×7) via step flow at room temperature by exciting the substrate with femtosecond laser pulses during pulsed laser deposition (PLD).<sup>11</sup> The growth process was attributed to the competition between the nonthermal laser-induced desorption of surface atoms and the adsorption of the other atoms.<sup>10,11</sup> Also, irradiation by a few hundred eV electron beams during deposition of CeO<sub>2</sub> on Si was reported to enhance epitaxy and reduce the required temperature for epitaxial growth from that without

electron irradiation by more than 100 °C.<sup>4</sup> We show that laser irradiation during the PLD of Ge on Si(100)-(2×1) enhances the crystallinity of quantum dots (QDs) and lessens the temperature required for their formation.

The self-assembly of Ge QD on Si has wide range of applications including midinfrared photodetectors,<sup>12</sup> thermoelectric devices,<sup>13</sup> and enhanced performance Si solar cells.<sup>14</sup> In such system, upon the completion of the 4–6 ML wetting layer, three-dimensional (3D) nucleation of Ge begins with the formation of faceted hut or pyramid clusters in order to minimize strain due to lattice mismatch.<sup>15</sup> As the film coverage increases, domes form on the expense of the hut clusters.<sup>16</sup> The facetation of the huts and domes depends on the deposition technique as well as the deposition conditions.<sup>17,18</sup>

Development of low temperature growth methods is of much interest in semiconductor fabrication. Lowering the epitaxial growth temperature is a key parameter to suppress the introduction of defects such as dislocations and stacking faults.<sup>19</sup> It has been shown that for Si–Ge the maximum epitaxial thickness without the introduction of any defects, referred to as critical thickness, is a function of the epitaxial growth temperature and the Ge mole fraction.<sup>20</sup> For example, for a 30% Ge concentration, the critical thickness at 500 °C is about five times that at 750 °C.<sup>20</sup> In addition, low temperature epitaxy prevents the alteration of the characteristics of devices already fabricated on the wafer. This is particularly critical for submicron structures with abrupt interfaces or sharp doping profiles.

We show that laser irradiation of the substrate during PLD of Ge on Si(100)-(2×1) reduces the epitaxial temperature. The low temperature epitaxy is shown to be induced by electronic excitation rather than thermal. In Sec. II, the experimental setup and conditions are given, and the results are discussed in Sec. III.

## II. EXPERIMENT

Ge on Si(100)-(2×1) was grown by PLD in an ultra-high vacuum (UHV) chamber, in which the Si substrate was

<sup>a)</sup>Electronic mail: helsayed@odu.edu.

heated by direct current. The Ge target was mounted on a rotated holder with a variable rotation speed. Target rotation during PLD reduces the formation of particulates. Before being loaded into the UHV chamber, the Si(100) substrates (dimensions of  $3.5 \pm 0.5 \times 10 \pm 0.5 \text{ mm}^2$ , *p*-type boron doped, resistivity  $0.060\text{--}0.075 \text{ } \Omega \text{ cm}$ ) were cleaned by chemical etching using a modification to the Shiraki method, as described previously.<sup>18</sup> The Ge target was a 2 in. disk, 0.5 mm thick undoped *n*-type with a resistivity of  $45\text{--}58.7 \text{ } \Omega \text{ cm}$ . The vacuum system was then pumped down, baked for  $>12 \text{ h}$ , and the sample is flashed to  $\sim 1100 \text{ }^\circ\text{C}$  in order for the  $(2 \times 1)$  reconstruction to form. Sample heating was done by passing direct current through it. The surface temperature was initially measured using a *K*-type thermocouple that was mechanically attached to the surface of the sample. A calibration curve relating the surface temperature obtained by the thermocouple and the sample conductivity was obtained and used for subsequent temperature measurement. This approach was used for temperature measurement in order to avoid complications due to changes in thermocouple properties by repeated flashing at high temperatures. We estimate that our temperature measurement accuracy is  $\pm 15\%$ , mainly limited by the accuracy of determining sample conductivity with temperature. The chamber pressure was maintained at  $<1 \times 10^{-9} \text{ Torr}$ .

A *Q*-switched Nd-doped yttrium aluminum garnet laser [wavelength 1064 nm, full width at half maximum (FWHM) of  $\sim 40 \text{ ns}$ , repetition rate of 50 Hz] was split into an ablation beam and an excitation beam of nonequal powers by means of a half wave plate and a polarizing beam splitter. The *p*-polarized ablation beam was focused on the rotating Ge target to a spot size of  $\sim 330 \text{ } \mu\text{m}$  (measured at  $1/e$  of the peak value), resulting in a laser fluence of  $\sim 4.9 \text{ J/cm}^2$ . The *s*-polarized excitation beam, however, was left unfocused with a beam diameter of  $\sim 5.8 \text{ mm}$  (measured at  $1/e$  of the peak value) and was used to irradiate the Si(100) substrate and the Ge film during deposition. A 12 keV reflection high-energy electron diffraction (RHEED) electron gun was used to monitor growth dynamics during deposition, while a phosphor screen displayed the electron diffraction pattern, which was recorded by means of a charge-coupled device camera. The electron beam had  $\sim 3^\circ$  angle of incidence with the surface of the Si(100) substrate. Postdeposition scanning tunneling microscopy (STM) was used to study the morphology of the grown films. The STM was operated in the constant voltage scan mode. The Ge films were grown on Si(100)- $(2 \times 1)$  at different substrate temperatures and different laser excitation conditions but with the same ablation laser fluence. The growth dynamics and morphology of the films grown under the laser excitation are compared to those grown at the same deposition conditions without laser excitation.

### III. RESULTS AND DISCUSSIONS

For PLD of Ge on Si(100) without laser excitation of the substrate, the Ge RHEED transmission diffraction patterns only show for samples grown above  $\sim 400 \text{ }^\circ\text{C}$ .<sup>18</sup> The appearance of RHEED transmission diffraction patterns indicates

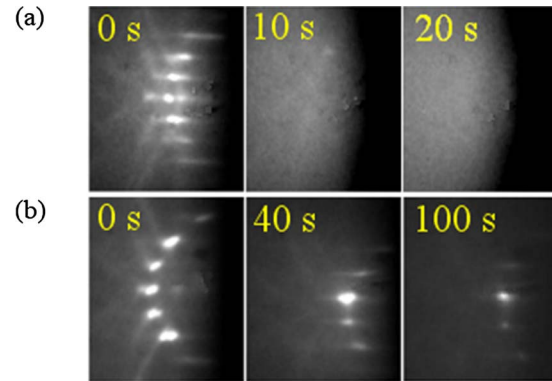


FIG. 1. (Color online) RHEED patterns recorded at different deposition times for two samples deposited at  $\sim 120 \text{ }^\circ\text{C}$  by ablation laser fluence of  $4.9 \text{ J/cm}^2$  and laser repetition rate of 50 Hz (a) without laser excitation and (b) with excitation laser energy density of  $130 \pm 52 \text{ mJ/cm}^2$ .

the formation of crystalline Ge QD, which starts by the formation of hut clusters that are faceted by different planes, depending on the cluster height.<sup>18</sup> For samples grown at substrate temperatures lower than  $\sim 400 \text{ }^\circ\text{C}$ , the intensity of the Si(100)- $(2 \times 1)$  RHEED spots decays continuously with deposition time until they completely disappear, resulting in a diffuse pattern, after a given thickness that increases with the substrate temperature. This indicates the formation of 3D structures that collectively lack long range order, as was confirmed by RHEED and atomic force microscopy.<sup>18</sup>

In order to study the effect of the laser-induced electronic excitations on the PLD of Ge on Si(100)- $(2 \times 1)$ , a set of samples was deposited under the same laser conditions but at a substrate temperature of  $\sim 120 \text{ }^\circ\text{C}$ . The RHEED patterns were recorded at different deposition times, as shown in Fig. 1. Under these conditions, all samples show continuous RHEED intensity decay until the complete disappearance of the patterns, as shown in Fig. 1(a). However, the time required for the disappearance of the RHEED pattern for the laser irradiated films shown in Fig. 1(b) is  $\sim 180 \text{ s}$  (corresponding to  $\sim 9 \text{ ML}$ ), which is approximately nine times that required for the nonirradiated samples ( $\sim 20 \text{ s}$  or  $\sim 1 \text{ ML}$ ), as shown in Fig. 1(a). The decay in the RHEED spots intensity and the increase in the background are associated with an increase in the film roughness. The faster the decay of the pattern, the rougher the surface will be. Therefore, laser irradiation of the substrate decreases the roughness of the film even though epitaxy is not achieved.

Next, we studied Ge growth on Si(100)- $(2 \times 1)$  at a substrate temperature of  $\sim 260 \text{ }^\circ\text{C}$  for 160 s (8000 pulses). Some of these samples were deposited without laser excitation while others were deposited with substrate excitation by laser pulses of different energy densities. The error range in the energy density arises from the alignment of the excitation laser on the substrate and the laser beam profile. Figure 2(a) shows the disappearance of the Si(100)- $(2 \times 1)$  RHEED pattern during the growth of a Ge film without laser excitation, while Fig. 2(b) shows an *ex situ* STM scan obtained over  $1.2 \times 1.2 \text{ } \mu\text{m}^2$  of the resulting film. The film could be described as a collection of 3D clusters characterized by the randomness in their shape, size, and spatial distribution. This is usually attributed to the slow surface diffusion of the ad-

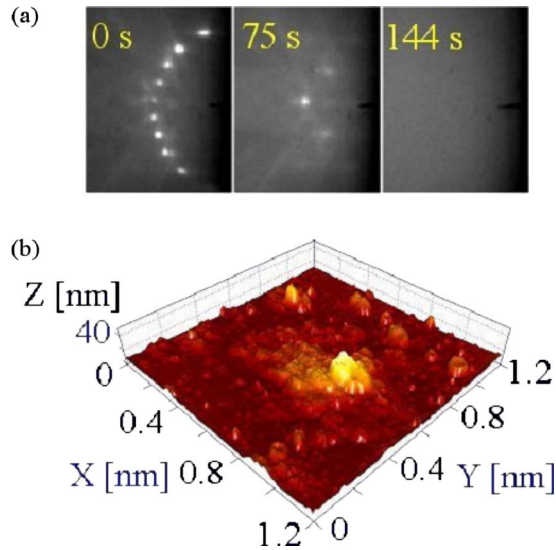


FIG. 2. (Color online) (a) RHEED patterns recorded at different deposition times for a sample grown without laser excitation at a temperature of  $\sim 260$  °C by ablation laser energy density of  $4.9$  J/cm<sup>2</sup> and laser repetition rate of  $50$  Hz. (b) 3D STM image of the final film.

sorbed atoms, which is expected at this relatively low temperature.

For PLD, *in situ* measurement of the film thickness by a crystal thickness monitor is not usually accurate due to the high directionality of the plume. Possible deviation of the energetic adatoms' sticking coefficient to the Au-coated crystal from that to the substrate could also present another complication. We have placed a crystal thickness monitor in the location of the substrate in separate PLD runs to estimate the deposition thickness per pulse. The average rate of deposition measured that way was  $(2.13 \pm 0.16) \times 10^{-3}$  Å/pulse. The error range considered only the standard deviation in repeated depositions and did not consider the variation in the sticking coefficient of Ge to the Au-coated crystal from that for Si, nor did it consider the plume nonuniformity over the  $50$  mm<sup>2</sup> area of the crystal thickness monitor. The thickness calibration was also performed by a spectroscopic ellipsometry (Woollam M44 ellipsometer). We used a model of a thin flat Ge layer on the  $0.5$  mm thick Si wafer. The average deposition rate in this case was found to be  $(1.34 \pm 0.06) \times 10^{-3}$  Å/pulse. The error range included was that from fitting the measured data to the assumed model considering the variation in the optical properties of the film from the bulk values. We rely on the thickness calibration by the ellipsometer because we believe it is more accurate than that obtained from the crystal thickness monitor.

Figure 3 shows the RHEED patterns for a sample grown under laser excitation with a fluence of  $144 \pm 58$  mJ/cm<sup>2</sup>. Initially, the substrate's  $(2 \times 1)$  RHEED pattern did not change during the first few seconds of deposition, which corresponds to the epitaxial growth of the wetting layer. After deposition for  $\sim 61$  s ( $\sim 3$  ML), the reflection RHEED pattern transformed into an elongated transmission pattern, thus, indicating the initial formation of the hut QD, as discussed in Ref. 18. As the film thickness was increased further, these spots became more intense before they became rounded in shape, indicating the formation of the dome QD.<sup>18</sup> Compari-

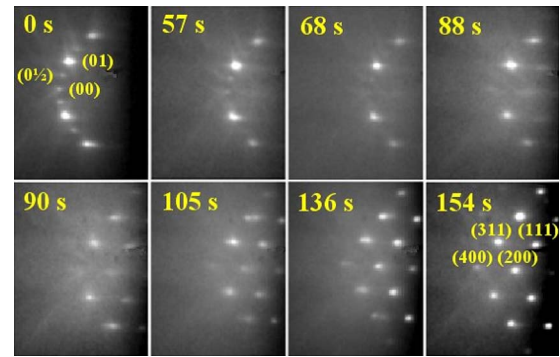


FIG. 3. (Color online) (a) RHEED patterns recorded at different deposition times for a sample grown with excitation laser energy density of  $144 \pm 58$  mJ/cm<sup>2</sup> at  $\sim 260$  °C with laser ablation fluence of  $4.9$  J/cm<sup>2</sup> and laser repetition rate of  $50$  Hz.

son of the surface morphology development with time under laser substrate excitation shows similar trends as observed without laser excitation but at a higher substrate temperature. For example, we previously reported that when the substrate was at  $400$  °C without laser excitation, the transition from reflection RHEED pattern to elongated transmission pattern occurs after depositing  $\sim 4$  ML.<sup>18</sup> Within the experimental accuracy, this is similar to the  $\sim 3$  ML transition coverage observed here for a substrate temperature of  $\sim 260$  °C but with laser substrate excitation at a fluence of  $144 \pm 58$  mJ/cm<sup>2</sup>. Moreover, the formation of the rounded transmission RHEED feature without laser excitation at  $400$  °C occurred at a coverage between  $\sim 9$ – $13$  ML (measured using a crystal thickness monitor), while with the laser excitation conditions above, the rounded RHEED features occurred after  $\sim 7$ – $8$  ML (measured by spectroscopic ellipsometry). As stated previously, ellipsometry measurement gave lower thickness than the crystal thickness monitor placed in the substrate location. Thus, the transition thickness to the rounded transmission RHEED feature without and with laser excitation at the different substrate temperatures used was similar within the experimental error.

Figure 4 compares the STM images of three samples grown for  $160$  s ( $\sim 8$  ML) for laser excitation energy densities of  $50 \pm 20$ ,  $87 \pm 35$ , and  $144 \pm 58$  mJ/cm<sup>2</sup>. The morphologies of the grown Ge QDs are domes, the majority of which has continuous round edges while a small fraction is multifaceted. The crystalline nature of these domes is evident from the RHEED patterns, as shown in Fig. 4. The length histograms of each STM image are shown. The size distributions for samples deposited with laser excitation using an energy density of  $50 \pm 20$  and  $87 \pm 35$  mJ/cm<sup>2</sup> are unimodal with most expected length (parallel to the substrate surface)  $L_m$  of  $10.4 \pm 0.3$  and  $10.7 \pm 0.2$  nm and FWHM of  $9$  and  $6$  nm, respectively. However, the size distribution for the sample deposited with  $144 \pm 58$  mJ/cm<sup>2</sup> excitation energy density is bimodal with  $L_m = 10.6 \pm 0.5$  and  $28.4 \pm 0.9$  nm with the corresponding FWHM of  $9$  and  $8$  nm. The small peak in the size distribution of Fig. 4(a) with  $L_m = 28.4 \pm 0.9$  nm shows significantly more QD morphologies of multifaceted domes compared to the majority of the QDs that are represented in the peak with  $L_m = 10.6 \pm 0.5$  nm. Comparing the STM images of the three samples in Fig. 4,

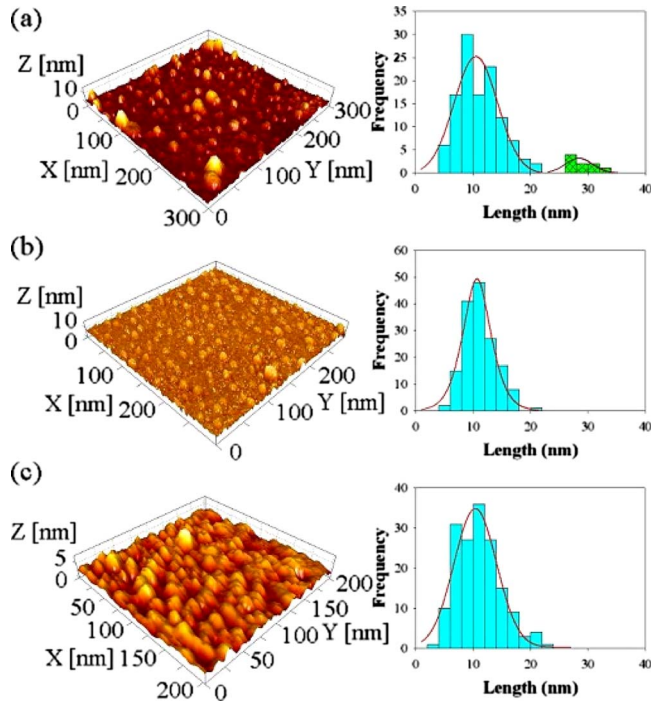


FIG. 4. (Color online) STM images and cluster length distributions for samples grown at  $\sim 260$  °C under laser ablation fluence of  $4.9$  J/cm<sup>2</sup> and laser repetition rate of  $50$  Hz for excitation laser energy density of (a)  $144 \pm 58$  mJ/cm<sup>2</sup> ( $d = 1.4 \times 10^{11}$  cm<sup>-2</sup>, CR  $\sim 11\%$  for lower size unimodal distribution and  $\sim 18\%$  for combined distributions), (b)  $87 \pm 35$  mJ/cm<sup>2</sup> ( $d = 1.7 \times 10^{11}$  cm<sup>-2</sup>, CR  $\sim 12\%$ ), and (c)  $50 \pm 20$  mJ/cm<sup>2</sup> ( $d = 4.1 \times 10^{11}$  cm<sup>-2</sup>, CR  $\sim 31\%$ ).

$L_m$  is about the same for the three samples if the higher length distribution is neglected. Cluster height statistics give values of the most expected heights of  $4$ ,  $7$ , and  $3$  nm and height FWHM of  $2$ ,  $2$ , and  $5$  nm for the samples in Figs. 4(a)–4(c), respectively. For the excitation energy density of  $144 \pm 58$  mJ/cm<sup>2</sup>, the coverage ratio (CR) (defined as  $\Sigma$  cluster areas/total scanned area) is  $\sim 11\%$  for the lower size unimodal distribution and  $\sim 18\%$  for the combined distributions. This becomes  $\sim 31\%$  when the excitation is decreased to  $50 \pm 20$  mJ/cm<sup>2</sup>. The corresponding cluster density  $d$  decreases with increased energy density from  $\sim 4.1 \times 10^{11}$  to  $\sim 1.4 \times 10^{11}$  cm<sup>-2</sup>.

The enhancement of QD crystallinity under laser excitation is not expected to be associated with a temperature rise due to laser absorption in the Si substrate. According to a one-dimensional heat diffusion model, similar to that discussed in Ref. 21, the maximum temperature rise due to the absorption of the  $1064$  nm excitation laser in the skin depth of Si ( $\sim 60$   $\mu$ m) is  $\sim 11$  °C for the highest laser energy density used in the present experiments. This temperature excursion decays to almost the substrate temperature in  $\sim 0.1$  ms. For Ge, the skin depth for wavelength  $1064$  nm is  $200$  nm and the maximum temperature rise, if bulk Ge is irradiated with the same laser energy density, is  $\sim 120$  °C. Even if we consider that the thin Ge layer might have different optical properties than bulk Ge in a way to enhance energy coupling to it, heat diffusion to the Si substrate will limit the temperature excursion time to  $< 0.1$  ms. This time scale is too short to affect the nucleation and growth mecha-

nism. Thus, for several monolayers of Ge on Si, the temperature excursion and its duration are too small to play a role in the much slower processes occurring on the surface that affect the growth mode. Thus, we conclude that the effect of laser excitation on the growth mode is nonthermal.

While direct laser surface heating is small to influence the growth of Ge on Si(100) and thus can be ruled out, the exact mechanism responsible for the enhancement of QD crystallinity under laser irradiation is not clear. Enhanced surface diffusion by a mechanism similar to that causing surface atom electronic desorption could be involved. The yield of the Si atoms, nonthermally removed via laser-induced electronic excitations, has been reported to (1) depend super-linearly on the laser energy density, (2) depend on the excitation wavelength, (3) be enhanced near pre-existing vacancies thus forming vacancy clusters, and (4) be enhanced near pre-existing defects for  $n$ -type surfaces compared to  $p$ -type surfaces.<sup>5,7,9</sup> The nature of vacancy generation depends on the surface with monovacancies almost exclusively formed on Si(111)-(7 $\times$ 7) (Ref. 22) while clustering occurs in Si(111)-(2 $\times$ 1),<sup>9</sup> InP(110)-(1 $\times$ 1), and GaAs(110)-(1 $\times$ 1).<sup>23</sup> Due to the low surface absorption coefficient of  $1064$  nm radiation in Si, photoexcitation takes place in the bulk,<sup>1</sup> resulting in a high density of electron-hole pairs that can transfer to the surface leading to charge redistribution and surface instability.<sup>7</sup> Hole localization onto particular surface sites results in selective bond breaking via a proposed THL mechanism.<sup>1,7</sup> In the THL mechanism, neutral atom desorption is induced by strong lattice relaxation associated with localization of two valence holes on a surface bond.<sup>24,25</sup> THL at a surface site affects the surface atom bonding weakening the bond and inducing a strong atom vibration.<sup>5</sup> Localization of the first hole on the surface causes a “defect site.” The second hole localization causes strong vibrations of the surface atom, which could lead to bond breaking. Consequently, these atoms are ejected due to this transient strong lattice vibration (phonon kick) with a distribution of translational energy that starts from a given onset.<sup>5</sup> Vibrational relaxation after electronic excitation would lead to many phonons being emitted. If the phonon kick perpendicular to the surface imparted to a surface atom is not sufficient to cause desorption, the enhanced vibrational motion could lead to increased surface diffusion. In growth of Ge on Si, increasing adatom diffusion affects the QD morphology in a way similar to that caused by increasing the substrate temperature. We cannot also rule out other mechanisms such as preferential desorption of Ge atoms from defect sites. Further studies are needed to elucidate the mechanism involved.

We note that previous studies lead to the conclusion that the effect of electronic excitation on thin film growth is not limited to laser excitation. It has been reported that substrate irradiation by an electron beam of energy of a few hundreds of eV during deposition of CeO<sub>2</sub> reduces the required temperature for epitaxial growth on Si(100) by more than  $100$  °C.<sup>4</sup> These electrons ionize surface atoms and adatoms enhancing adatom diffusion toward lattice sites via Coulomb interaction.<sup>4</sup> Electron beam irradiation was also found to increase the epitaxial recrystallization rates in amorphous SrTiO<sub>3</sub> by orders of magnitude compared to thermal effects.<sup>2</sup>

A mechanism was proposed based on localized excitations affecting local atomic bonds by lowering the energy barrier to defect recovery.<sup>2</sup>

The present results show that surface electronic excitation can be effectively used to alter the growth mode and produce low temperature epitaxy. Laser substrate excitation affects the PLD growth of Ge QD on Si(100)-(2 × 1). Electronic excitation by laser irradiation of the substrate changes film morphology and reduces the temperature required for the formation of crystalline QD. Thermal effects are not responsible for these observations. We postulate that enhanced surface diffusion by a mechanism similar to that causing surface atom electronic desorption could be involved.

## ACKNOWLEDGMENTS

This material is based on work supported by the U.S. Department of Energy, Division of Material Sciences under Grant No. DE-FG02-97ER45625 and the National Science Foundation (Grant No. DMR-0420304). The authors would like to thank Dr. Z. Guo of Old Dominion University for helping to conduct the ellipsometry measurements.

<sup>1</sup>K. Tanimura, E. Inami, J. Kanasaki, and W. P. Hess, *Phys. Rev. B* **74**, 035337 (2006).

<sup>2</sup>Y. Zhang, J. Lian, C. M. Wang, W. Jiang, R. C. Ewing, and W. J. Weber, *Phys. Rev. B* **72**, 094112 (2005).

<sup>3</sup>N. Itoh and A. M. Stoneham, *J. Phys.: Condens. Matter* **13**, R489 (2001).

<sup>4</sup>T. Inoue, Y. Yamamoto, and M. Satoh, *J. Vac. Sci. Technol. A* **19**, 275

(2001).

<sup>5</sup>J. Kanasaki, K. Iwata, and K. Tanimura, *Phys. Rev. Lett.* **82**, 644 (1999).

<sup>6</sup>A. M. Stoneham and N. Itoh, *Appl. Surf. Sci.* **168**, 186 (2000).

<sup>7</sup>J. Kanasaki, K. Katoh, Y. Imanishi, and K. Tanimura, *Appl. Phys. A: Mater. Sci. Process.* **79**, 865 (2004).

<sup>8</sup>B. R. Trenhaile, V. N. Antonov, G. J. Xu, K. S. Nakayama, and J. H. Weaver, *Surf. Sci.* **583**, L135 (2005).

<sup>9</sup>E. Inami and K. Tanimura, *Phys. Rev. B* **76**, 035311 (2007).

<sup>10</sup>V. A. Fedotov, K. F. MacDonald, N. I. Zheludev, and V. I. Emel'yanov, *J. Appl. Phys.* **93**, 3540 (2003).

<sup>11</sup>I. El-Kholy and H. E. Elsayed-Ali (unpublished).

<sup>12</sup>M. S. Hegazy, T. F. Refaat, M. Nurul Abedin, and H. E. Elsayed-Ali, *Opt. Eng.* **44**, 059702 (2005).

<sup>13</sup>J. L. Liu, A. Khitun, K. L. Wang, T. Borca-Tasciuc, W. L. Liu, G. Chen, and D. P. Yu, *J. Cryst. Growth* **227–228**, 1111 (2001).

<sup>14</sup>A. Alguano, N. Usami, T. Ujihara, K. Fujiwara, G. Sazaki, K. Nakajima, and Y. Shiraki, *Appl. Phys. Lett.* **83**, 1258 (2003).

<sup>15</sup>V. Cimalla, K. Zekentes, and N. Vouroutzis, *Mater. Sci. Eng., B* **88**, 186 (2002).

<sup>16</sup>O. G. Schmidt, C. Lange, and K. Eberl, *Appl. Phys. Lett.* **75**, 1905 (1999).

<sup>17</sup>F. Montalenti, P. Raiteri, D. B. Migas, H. Von Känel, A. Rastelli, C. Manzano, G. Costantini, U. Denker, O. G. Schmidt, K. Kern, and L. Miglio, *Phys. Rev. Lett.* **93**, 216102 (2004).

<sup>18</sup>M. S. Hegazy and H. E. Elsayed-Ali, *J. Appl. Phys.* **99**, 054308 (2006).

<sup>19</sup>N. Tamura and Y. Shimamune, *Appl. Surf. Sci.* **254**, 6067 (2008).

<sup>20</sup>D. C. Houghton, *J. Appl. Phys.* **70**, 2136 (1991).

<sup>21</sup>X. Zeng and H. E. Elsayed-Ali, *Phys. Rev. B* **64**, 085410 (2001).

<sup>22</sup>J. Kanasaki, T. Ishida, K. Ishikawa, and K. Tanimura, *Phys. Rev. Lett.* **80**, 4080 (1998).

<sup>23</sup>T. Gotoh, S. Kotake, K. Ishikawa, J. Kanasaki, and K. Tanimura, *Phys. Rev. Lett.* **93**, 117401 (2004).

<sup>24</sup>H. Sumi, *J. Phys. C* **17**, 6071 (1984).

<sup>25</sup>H. Sumi, *Surf. Sci.* **248**, 382 (1991).